Pergamon

PII: S0191-8141(96)00089-2

Journal of Structural Geology, Vol. 19, Nos 3-4, pp. 397 to 411, 1997

0191-8141/97 $17.00 + 0.00

Geomorphic evidence for tear faults accommodating lateral propagation of an active fault-bend fold, Wheeler Ridge, California

KARL MUELLER*

Department of Geological and Geophysical Sciences, Princeton University, Princeton, NJ 08544, U.S.A.

and

PETER TALLING

Department of Geology, Bristol University, Bristol BS8 1RJ, U.K.

(*Received* 2 *February* 1996; *accepted in revised form* 10 *October* 1996)

Abstract—Wheeler Ridge is the topographic expression of an actively growing fault-bend fold developed in the hanging walls of a system of mostly north-vergent blind thrusts. The eastern tip of the fold system has migrated laterally by approximately 3 km during the last 120 ka perpendicular to the regional shortening direction. Comparison of surface topography and structural cross-sections indicates that eastern Wheeler Ridge comprises three fold segments, whose topographic expression steps southward towards the eastern end of the structure. Lateral propagation of the fold is associated with numerous tear faults, expressed as fault scarps that face towards the eastern end of the fold. We suggest that these tear faults accommodate earthquake-related processes that collectively build plunge of the fold and lateral propagation on blind thrusts. We envisage that the fold will grow primarily by thrust faulting events with similar displacement(s) along strike that are terminated abruptly at tear faults, build displacement over multiple earthquake cycles and then step eastward to form a new tear fault. Formation of especially large tear faults is inferred to be in response to an increase in rock strength governed by lithology. The high fault displacement vs length (D/L) for Wheeler Ridge may be related to high strain rates across a restraining bend in the nearby San Andreas strike-slip fault system.

INTRODUCTION

Measurements of the dimensions of dip-slip fault populations within deforming areas indicate that fault length increases with greater displacement, or by linkage of separate fault segments (Walsh and Watterson, 1988; Gillespie *et al.*, 1992; Cowie and Scholz, 1992a; Dawers *et al.*, 1993; Trudgill and Cartwright, 1994). These studies predict that fault tips migrate laterally in a direction perpendicular to the regional extension direction as displacement accumulates. Field studies which document lateral migration of individual faults are, however, very rare (Jackson and Leeder, 1994; Jackson *et al.*, 1996; Stewart, 1996). Wheeler Ridge has been shown to result from fault-bend folding in the hanging wall of an active thrust system (Medwedeff, 1992) based on studies using tightly-spaced borehole data from oilfields. Detailed subsurface mapping from this work, coupled with absolute and relative dating of deformed alluvial surfaces on the crest of the fold (Keller *et al.*, 1989; Zepeda *et al.*, 1996), has demonstrated lateral growth of the structure during the last ~250 ka.

We combine these earlier studies with a geomorphic analysis of the well-preserved topography of the fold crest and exposures in transverse river valleys to document structures which act to build the fold in three dimensions. Wheeler Ridge is uniquely suited for study of the lateral growth of fault-related folds because well-preserved geomorphic surfaces, fault scarps and subsurface structural mapping can be combined to define a progressive folding history for at least the last 125 ka. Our aims are to: (1) document the structures that accommodate lateral fold growth, (2) further our understanding of the processes involved in fault-tip migration and (3) evaluate existing models of the fault geometry underlying the Wheeler Ridge (Medwedeff, 1992).

REGIONAL SETTING

Wheeler Ridge is located at the southern end of the San Joaquin Valley in central California (Fig. 1). The ridge exhibits up to 350 m of topographic relief and extends for ~10 km along strike (Fig. 2a). Fault-bend folding in the hanging wall of the Wheeler Ridge thrust accommodated uplift of the ridge, which is actively propagating northward and eastward for the portion of the structure we studied (Medwedeff, 1988; Zepeda *et al.*, 1996). Wheeler Ridge is the frontal fold in the Transverse Ranges thrust system, which has developed in response to shortening across a restraining bend in the San Andreas fault (Namson and Davis, 1988; Medwedeff, 1992; Zepeda *et al.*, 1996). North of Wheeler Ridge, blind thrust faults comprising the Coast Range thrust system have also produced a series of anticlinal folds oriented subparallel

*Present address: Department of Geological Sciences, University of Colorado, Boulder, CO 80309, U.S.A.

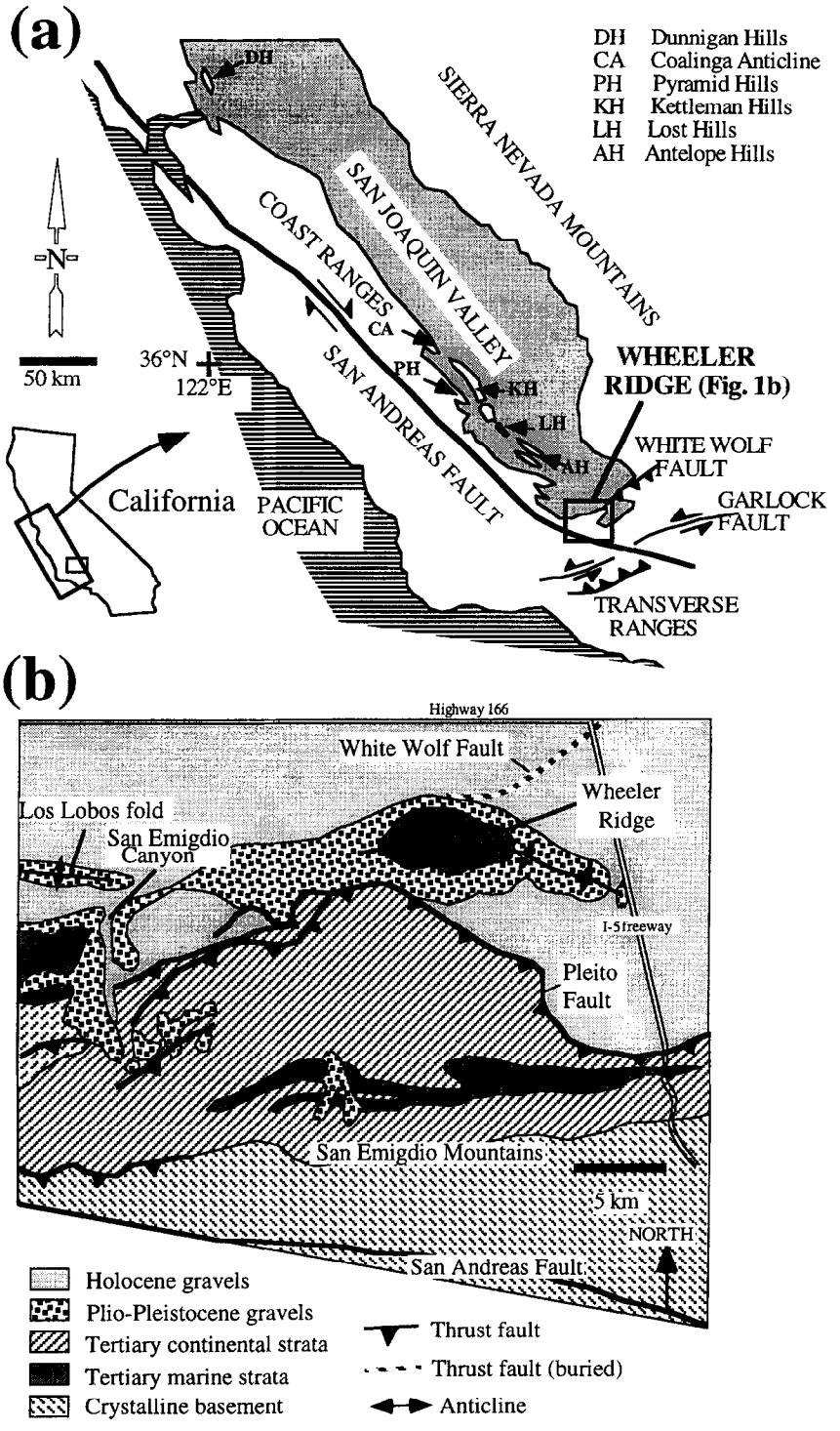

Fig. 1. (a) Map of central California showing the major tectonic features in the vicinity of the Wheeler Ridge. Anticlinal folds produced by blind thrusts comprising the Coast Range thrust system are indicated by letters. (b) Detailed geological map of the Wheeler Ridge and adjacent features referenced in the text.

to the San Andreas fault (Fig. 1b; Medwedeff, 1989; Ekstrom *et al.*, 1992; Stein and Ekstrom, 1992; Unruh and Moores, 1992; Bloch *et al.*, 1993). The Wheeler Ridge thrust fault, and the Pleito thrust to which it is linked to the south, are part of a thin-skinned fault system which deforms the upper 2–4 km of sedimentary strata in the southern San Joaquin Valley (Fig. 1; Medwedeff, 1992). Other active structures in this region include the White Wolf fault, a basement-involved thrust which extends from 17 km depth. Rupture on this deeper, basement-involved thrust resulted in the 1952 M7.6 Arvin–Tehachepi earthquake, which caused minor surface uplift in the vicinity of the ridge itself (Stein *et al.*, 1988).

The onset of uplift of Wheeler Ridge occurred before

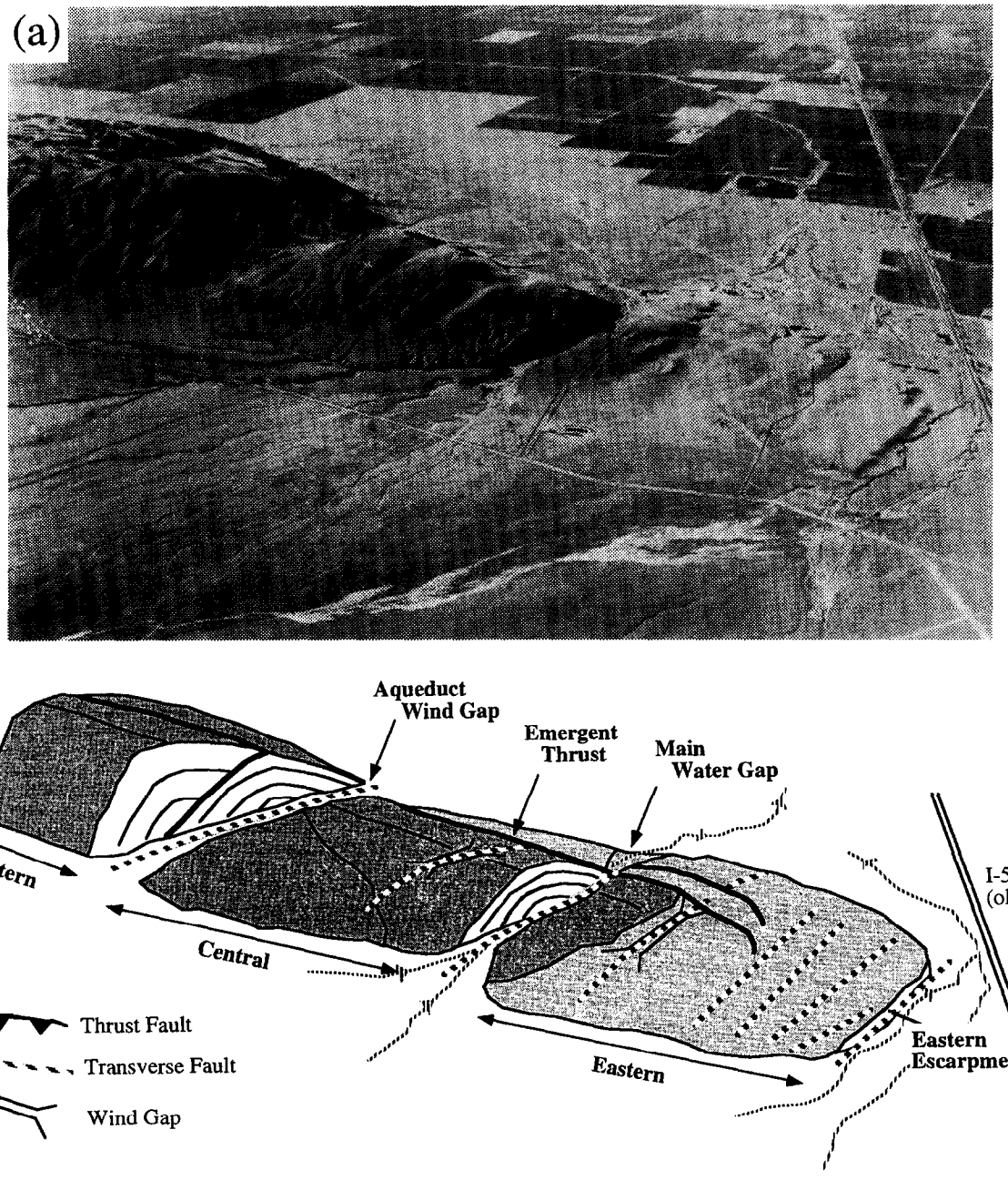

Fig. 2. (a) Aerial photograph from Shelton (1966) of eastern Wheeler Ridge anticline. The view is from the south-east across the rear of the ridge and out over the San Joaquin Valley. (b) Interpretative sketch of the Wheeler Ridge showing the terms used to describe locations on the ridge. The three major parts of the ridge (western, central and eastern) are separated by the aqueduct wind gap and main water gaps. A second wind gap is visible across the central part of the ridge. The escarpment near the eastern terminus of the ridge was produced by an oblique tear fault. Changes in drainage development on different parts of the ridge, which become progressively younger towards the east, are clearly shown in the photograph. Surfaces on the three distinct anticlinal folds which comprise the ridge are separately shaded. Note the tear faults which extend across the crest of the fold on the eastern segment.

~250 ka, continued at least to 1–7 ka and is likely active today (Keller *et al.*, 1989; Zepeda *et al.*, 1996). To the south-east of Wheeler Ridge (Figs 1 & 2a), the Pleito thrust offsets beds are dated using radiocarbon techniques as 300–1500 ybp (Hall, 1984). Deformation is thus occurring coevally on the Pleito and Wheeler Ridge thrusts. Work in the vicinity of San Emigdio Canyon, located 25 km west of Wheeler Ridge (Fig. 1), shows that deformation initiated on the Pleito thrust in the Mid-Pleistocene, and then migrated eastwards to the buried trace of the Wheeler Ridge fault (Keller *et al.*, 1989; Zepeda *et al.*, 1996). Forward propagation of the thrust belt into undeformed strata of the southern San Joaquin Valley has continued with the uplift of the Los Lobos folds during the last 5 ka (Keller *et al.*, 1989; Fig. 1).

TIMING OF FOLDING

Relative and absolute dating of geomorphic surfaces on Wheeler Ridge (Keller *et al.*, 1989; Zepeda *et al.*, 1996) has unambiguously shown that the eastern end of the fold has migrated towards the east. These data are important because they allow rates of forward and lateral propagation of Wheeler Ridge to be defined and correlated with the geometry of tectonically produced landforms, such as fold limbs, plunge panels and fault scarps, that result from these processes.

Medwedeff (1992) determined that the tip of Wheeler Ridge has migrated 2670 m in 117 ka at an average rate of 22.8 m ka^{-1}. Because this calculation defines the rate at which we interpret tear faults to form, the limitations of the age constraints used are discussed. In the following discussion the topographic surface of the ridge is divided into three parts (Figs 1 & 2b; western, central and eastern). The aqueduct wind gap, through which the California aqueduct flows, divides the western and central parts of the ridge. The central and eastern parts of the ridge are separated by a major water gap (the 'main water gap'). The eastern portion of the fold is bounded by the eastern escarpment (Medwedeff, 1992) a prominent east-facing fault scarp that displaces Holocene sediments.

Keller *et al.* (1986, 1989) and Zepeda *et al.* (1996) used radiocarbon techniques to date geomorphic surfaces on Wheeler Ridge and developed a soil chronosequence calibrated with another well-dated soil series in the San Joaquin Valley (Harden, 1982). Using the radiocarbon technique on detrital charcoal, the relatively undeformed alluvial fan lying east of the eastern branch of Salt Creek (Fig. 2a) was determined to be younger than 7 ka in age (Keller *et al.*, 1989). The degree of soil development in this deposit however, suggested that the charcoal sample had been reworked, and that the actual age of the surface is ~ 1 ka (Zepeda *et al.*, 1996).

Two radiocarbon dates, from pedogenic carbonate rinds on gravel clasts, yielded an age of 9 ± 3 ka for the eastern end of the youngest part of the ridge (Fig. 3). It is estimated that ~ 5 ka is needed to form such rinds (Seaver, 1986). An age of 14 ± 3 ka is thus determined for this surface (Keller *et al.*, 1989; Zepeda *et al.*, 1996; Fig. 4). Soils formed further west along more uplifted portions on the crest of Wheeler Ridge are better developed as indicated by an increase in rubification, and their clay and carbonate content (Keller *et al.*, 1989; Zepeda *et al.*, 1996). The ages of these folded alluvial deposits on the central and western parts of the ridge (Fig. 4) were estimated using an uplift rate derived from the adjusted radiocarbon date of 14 ± 3 ka and by comparison with other similarly developed and independently dated soil sequences in the San Joaquin Valley (Harden, 1982).

We assume that the relief of 24 m between the recent fan surface and the 14 ka surface represents a constant uplift rate of 1.7 ± 0.3 mm yr^{-1}. This rate was extrapolated to estimate that the eastern, central and western parts of the ridge were, respectively initially uplifted between 10 and 65 ka, 150 and 100 ka, and 250 and 200 ka (Zepeda *et al.*, 1996; Fig. 4). At present, there are no absolute age constraints for surfaces older than 14 ± 3 ka. Uncertainties in the single, adjusted radiometric age of 14 ka used to generate the uplift rate of 1.8 mm yr^{-1}, as well as fluctuations in uplift rates, will affect the accuracy of the ages assigned to surfaces on the ridge. The long-term rates of uplift appear to be broadly constant however, based on the comparison with other, better dated soil chronosequences in the San Joaquin Valley (Harden, 1982) which are typically accurate to $\pm$ 25% (Birkeland, 1984). In addition, studies of growth sediments deformed by active fault-bend folds in the offshore Santa Barbara Channel indicate that slip rates for some blind thrusts in southern California are nearly constant over long periods (Shaw and Suppe, 1994). The age constraints at Wheeler Ridge are thus useful for constraining the large-scale evolution of the ridge, and estimating the frequency of tear fault formation (~ 10–20 ka). They are not however, sufficiently precise to document short term (< 10 ka) patterns of fault-tip migration.

SUBSURFACE FAULT GEOMETRY

Medwedeff (1992) presented a detailed structural interpretation of thrust fault geometry underlying Wheeler Ridge based on subsurface data. A series of 17 horizons were correlated between a dense array of wells using spontaneous potential and resistivity logs. On the basis of these correlations he generated a series of seven line-balanced structural cross-sections, five of which crossed the eastern and central parts of the Wheeler Ridge (Figs 3 & 5). The central segment of Wheeler Ridge was interpreted to be formed above a wedge thrust, in which displacement is transferred to the south along a north-dipping fault (Fig. 5). This was based on the lack of obvious thrust-related shortening north of Wheeler Ridge (Medwedeff, 1992) and the upward increase in structural relief in the fold, which indicated that a second, south-vergent thrust ramp was present. Another south-dipping thrust was also mapped as offsetting strata in the uppermost part of the fold that ruptured the surface along the front limb of Wheeler Ridge, immediately east of the aqueduct wind gap. The subsurface geometry of much of the eastern segment of Wheeler Ridge was also mapped as a north-vergent thrust wedge. However, an abrupt change in fault geometry was interpreted to occur in the easternmost part of the fold, where the basal, south-dipping thrust extended to the surface without the associated north-dipping backthrust (Medwedeff, 1992).

Faults that traverse the fold were also documented by Medwedeff's (1992) cross-sections and structure contour maps (Figs 5 & 6). These faults are largely contained in the hanging wall of the basal, south-dipping thrust and display vertical separation that is down to the east. One

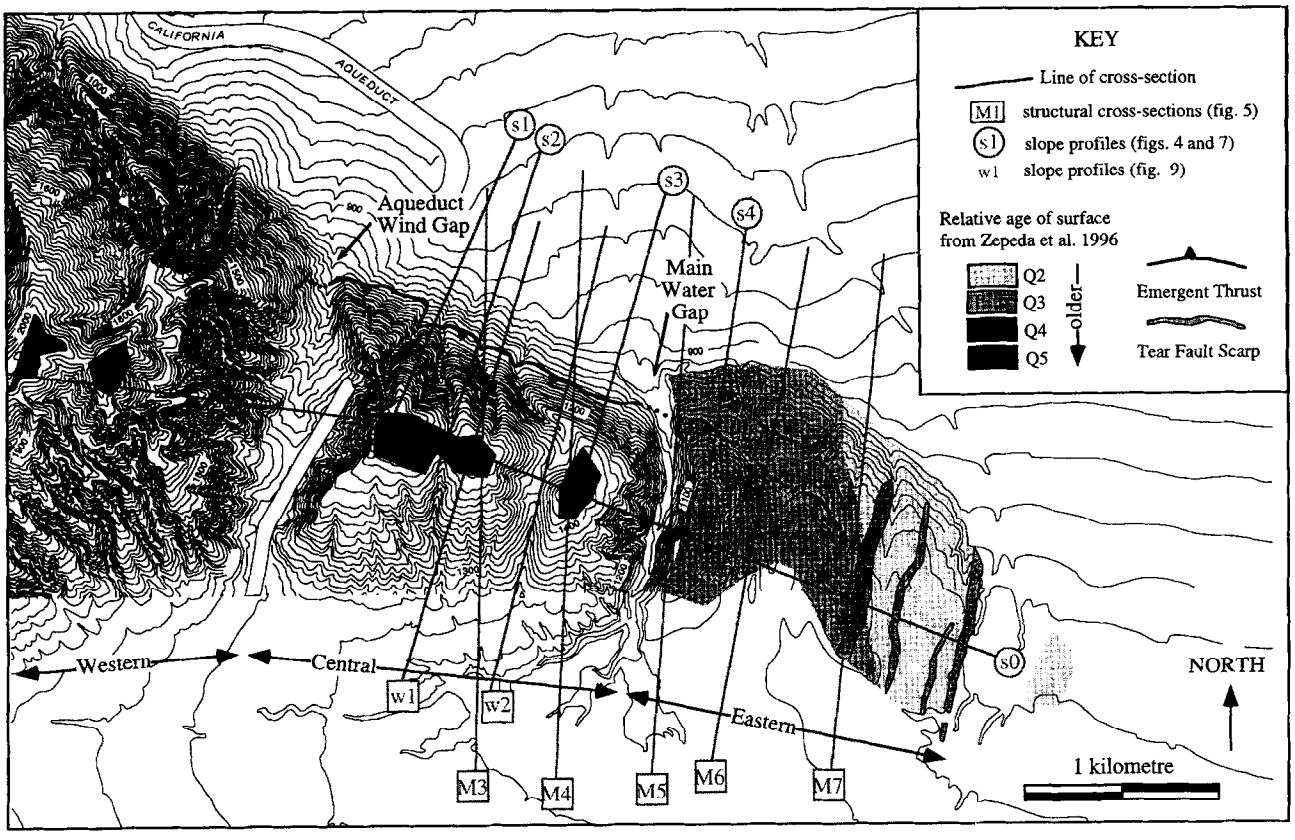

Fig. 3. Enlargement of a U.S.G.S. 1:24,000 scale topographic map showing the major structural and geomorphic features of the eastern part of the Wheeler Ridge. The locations of topographic cross-sections comprising Figs 7 and 9 are shown, together with the location of the structural cross-sections of Medwedeff (1992) (Fig. 5). M4 refers to Medwedeff's section 4 (Fig. 5), M5 refers to his section 5, etc. Note the change in contour interval from 20 to 40 feet in the lower portion of the figure.

fault that coincides with the location of the main water gap appears to accommodate northward offset of the eastern fold segment (Figs 2a & 6). Geomorphic features which traverse the fold, such as the aqueduct wind gap, main water gap, east-facing fault scarps and other minor wind gaps correspond to the location of the tear faults mapped in the subsurface by Medwedeff (1992) and provide important constraints on processes than govern lateral propagation.

GEOMORPHOLOGY

Emergent thrust faults

Two emergent thrust faults are exposed along the front limb and crest of Wheeler Ridge that accommodate shortening in the structurally highest levels of the fold. Subsurface mapping by Medwedeff (1992) (see his section 3) identified a south-dipping thrust that cuts the ground surface along the front limb of the fold immediately east of the aqueduct wind gap. Mapping of alluvial deposits in this area (Mueller and Suppe, 1997; Fig. 3) identified the trace of the thrust as an abrupt, sharp increase in slope partway up the fold limb (Fig. 7). The oversteepened part of the fold limb was interpreted to form by collapse of strata in the hanging wall of the emergent thrust onto the existing front limb, which formed above the blind north-vergent wedge thrust developed at a deeper level (Mueller and Suppe, 1997). The emergent, south-dipping thrust is exposed along the length of the front limb which forms the central segment of Wheeler Ridge (Figs 3, 5 & 7). It crosses the main water gap at a point midway up the front limb and extends eastward along the flat crest of the eastern segment of the fold. The trace of the thrust forms a distinct south-side-up scarp where it extends across the flat-lying crest of the eastern segment of the fold (Fig. 3).

We mapped the trace of the emergent, south-dipping thrust using 1:20,000 scale aerial photographs taken in 1952 (Fig. 3), prior to the excavation of a large gravel quarry now located along the front limb of the eastern segment of the fold. This fault was identified by Zepeda *et al.* (1991, 1996; Fig. 3) in the quarry where it was subsequently excavated in the center of the eastern part of the ridge. The fault exposure in the quarry dips 24° to the south and trends E–W, and has an offset of 2.5 m at the surface (Zepeda *et al.*, 1991, 1996). Although suggested by Zepeda *et al.* (1991, 1996) as such, this is not the primary south-dipping fault identified in the subsurface by Medwedeff (1992) on his section 7. The

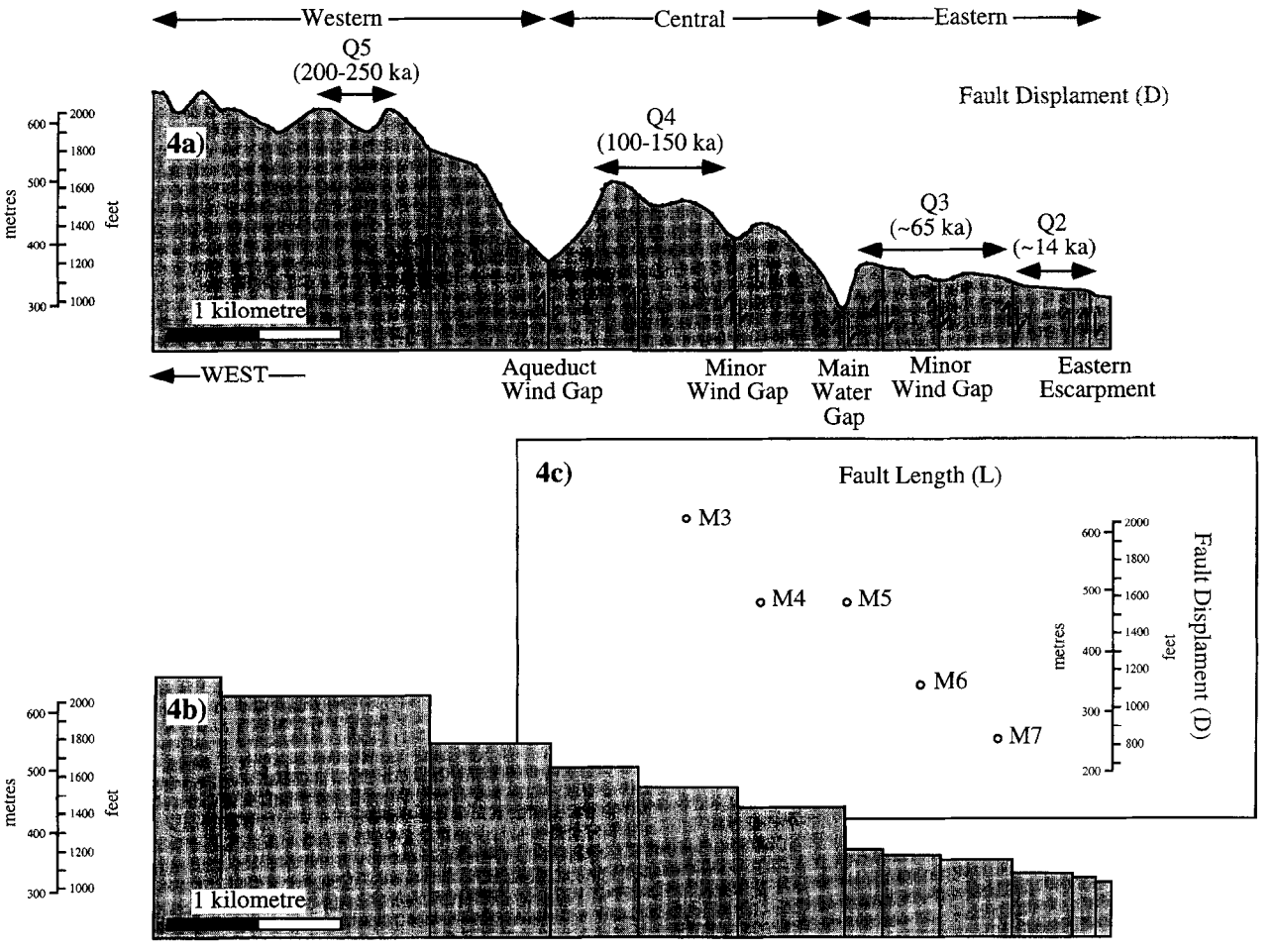

Fig. 4. (a) Vertically exaggerated topographic cross-section, oriented parallel to the crest of the ridge (after Zepeda *et al.*, 1996). The ages of surfaces on the ridge are those given by Zepeda *et al.* (1996). The inferred positions of major tear faults are indicated, together with the location of wind and water gaps. (b) Vertically exaggerated topographic cross-section, oriented in same location as (a), that illustrates the uneroded topography of the ridge, constructed by projection of plunge panel segments across known tear faults. (c) Graph illustrating the relationship between fault displacement, measured across the top of the ramp in the basal north-vergent thrust, with the location of cross-sections by Medwedeff (1992) along the strike of the fold, where the values were calculated. Note the step-like character of the profile between sections M4 and M5 in comparison to the location of tear faults shown on (b).

fault in the quarry cuts the surface 300 m to the south of the surface rupture shown by Medwedeff (1992) and the obvious north-facing front limb; also the south-dipping thrust studied in the quarry has about 2.5 m of dip-slip separation, much less than the 250 m of dip-slip displacement shown on the section by Medwedeff (1992), consistent with the width of the front limb.

Constraining the absolute timing of motion on the emergent, south-dipping thrust fault that extends along the front limb of Wheeler Ridge is difficult, because of the lack of well-dated young deposits deformed in the central part of the fold. However, the emergent, south-dipping thrust offsets deposits immediately east of the aqueduct wind gap which have soil profiles developed on them that correspond to the 65 ka Q3 surfaces (Mueller and Suppe, 1997) defined on the fold crest further east by Zepeda *et al.* (1991, 1996; Fig. 3). The fault also offsets 14 ± 3 ka Q2 deposits on the crest of the eastern portion of the fold that are constrained by radiocarbon dating of pedogenic carbonate. The fault does not offset Holocene (Q1 or historic?) sediments deposited in the mouth of the water gap; similarly it does not cut Q1 deposits mapped along the downthrown side of the eastern escarpment (Zepeda *et al.*, 1991, 1996). The emergent south-dipping thrust appears to die out midway across the eastern fold segment. These age constraints are consistent with either: (1) eastward propagation of the emergent thrust during the late Quaternary from ~ 125 ka to after 14 ± 3 ka, or (2) the emergent thrust postdates 14 ± 3 ka deposits all along its length.

The other emergent fault we mapped on Wheeler Ridge is a north-dipping thrust that extends for ~ 1000 m along strike along the front limb of the eastern segment of the fold. The thrust is mapped on archival airphotos (Fig. 3) taken prior to the excavation of the gravel quarry as a moderately dissected north-side-up

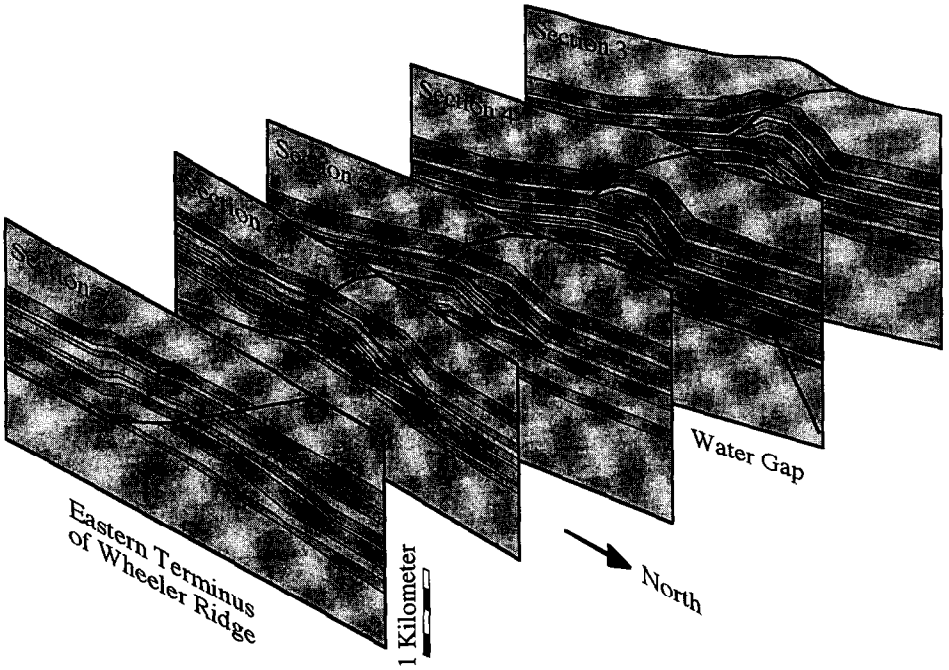

Fig. 5. Perspective series of cross-sections after Medwedeff (1992). Note the location of the emergent, south-dipping thrust which we interpret to be present based on mapping of landforms along the fold. Sections 3 and 4 cross the central part of the ridge. Section 5 is in the main water gap, whilst sections 6 and 7 cross the eastern part of the ridge. The location of sections is shown on Fig. 3.

scarp that is eroded by young drainages incised into the front limb of the fold. The north-dipping thrust is now well exposed in the 50-m high wall of the gravel quarry where it dips ~30° to the north and displays ~35 m of dip-slip displacement.

Plunge panel

The plunge panel of Wheeler Ridge is defined as the group of adjacent alluvial surfaces that collectively make up the flat-lying crest of the fold between its north- and south-dipping limbs (Figs 2a, 3, 4 & 8). Individual segments of the plunge panel are expressed as flat-lying geomorphic surfaces that increase in width (Fig. 8) and decrease in degree of incision from west to east (Fig. 2). Segments of the plunge panel located on the central part of Wheeler Ridge are ~250–300 m wide, underlain by 125 ka soils (Zepeda *et al.*, 1991, 1996; Fig. 4), and lie between deeply incised fold limbs. Although highly eroded here, at least three separate geomorphic surfaces comprise the plunge panel on the central part of the ridge, which are separated by two highly eroded, ~30 and 40 m high, east-facing steps interpreted to be fault scarps.

The plunge panel on the eastern part of Wheeler Ridge broadens abruptly across the main water gap and again across another minor wind gap located 500 m to the east (Figs 2a, 3 & 8). The segment of the fold crest immediately east of the main water gap is ~500 m wide, whereas the fold segment east of the minor wind gap is ~650 m wide. This portion of the plunge panel is flat-lying and largely undissected except for shallowly incised drainages on the front limb that are retreating headwards (Fig. 3).

The step-like nature of the plunge panel is reflected both by the uneroded, flat-lying geomorphic surfaces and well-preserved tear fault scarps which comprise the crest of the fold on the eastern portion of Wheeler Ridge (Figs 2c & 4b), and flat-lying strata exposed in the upper portions of quarry walls in the same region. Also, cross-sections M4 and M5 by Medwedeff (1992) west of the main water gap that lie on the same fold segment (i.e. between two east-facing fault scarps) illustrate similar amounts of shortening caused by fault slip along strike. We interpret these relationships to indicate that abrupt decreases in slip along the basal blind thrust occurs across tear faults, and not between them (i.e. the tear faults accommodate the decrease in shortening along strike; see also Fig. 4c).

The average elevation of the plunge panel also varies from west to east (Fig. 8). Although the plunge panel is deeply dissected west of the aqueduct wind gap, a low gradient surface is apparent when highpoints along the fold crest are connected (see section S0 on Figs 3 & 4). The plunge panel steepens markedly at the aqueduct wind gap along the central portion of the ridge until it reaches the main water gap (Fig. 4a & b). East of the main water gap, the plunge panel flattens to a lower average gradient.

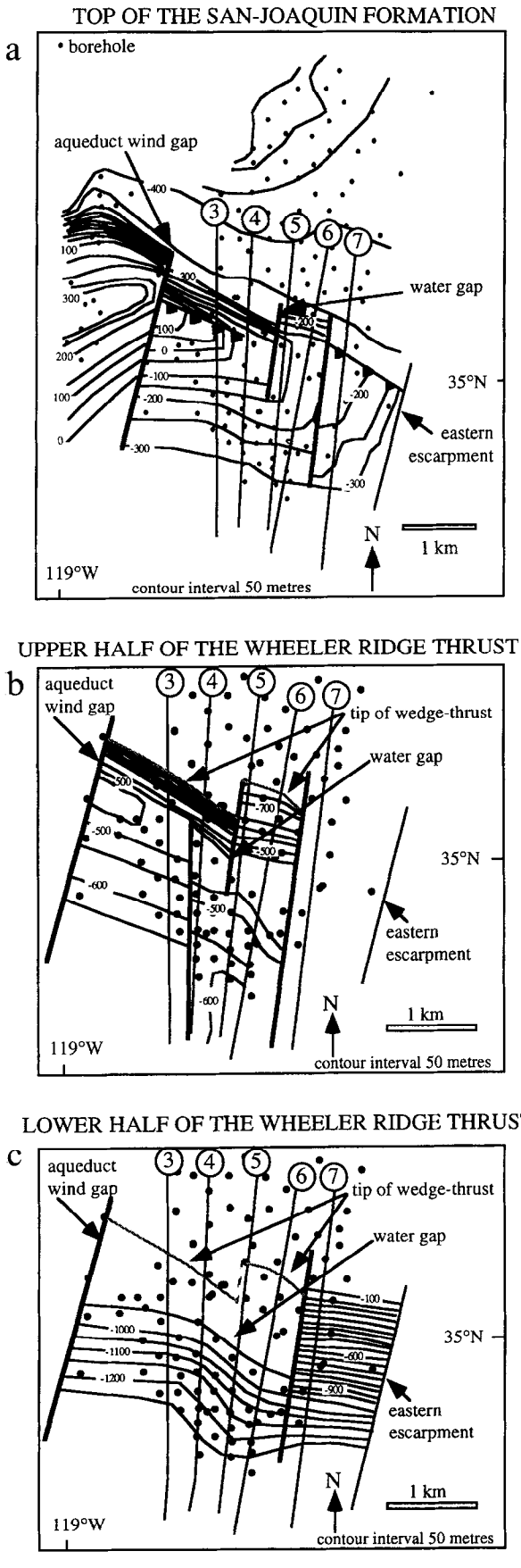

Fig. 6. Structure contour maps from Medwedeff (1992) illustrating the subsurface geometry of major tear faults and their coincidence with wind and water gaps.

East-facing fault scarps

Steps in surface topography evident on 1:24,000 scale maps and aerial photographs and subsurface structure contours (see figs 1.13 and 1.14 of Medwedeff, 1992) define numerous steeply-dipping NNE–SSW-trending faults (Figs 2a, 3, 4 & 8). These faults do not laterally offset the plunge panel of the fold and display vertical displacements that range from ~6 to 80 m (Fig. 8). In all cases these faults face eastward towards the termination of the fold. Faults with particularly large offsets underlie both the aqueduct wind gap and water gap, and the minor wind gap located on the central part of the fold.

These faults are best preserved on the eastern portion of Wheeler Ridge, where they extend across the plunge panel, subdividing it into several segments (Fig. 2c). In this location they are sharply defined and are only shallowly dissected by narrow rills and gullies. These faults terminate southward at the top of the back limb. The east-facing faults are not recognizable as linear scarps west of the main water gap where the fold is more deeply incised and eroded. The best preserved scarp on Wheeler Ridge is the eastern escarpment (Zepeda *et al.*, 1991, 1996; Medwedeff, 1992), a 24 m high scarp that bounds the eastern end of the fold.

Wind and water gaps

Three wind gaps of varying depth are preserved across the fold and include the aqueduct wind gap and smaller gaps across the central and eastern parts of the fold (Fig. 2a). The wind gaps are expressed as depressions in the ridge crest (Fig. 4) that resemble hanging valleys. These features have been interpreted to be formed by antecedent river valleys that once traversed the fold (Shelton, 1966; Zepeda *et al.*, 1991, 1996; Medwedeff, 1992). All three wind gaps coincide with either the location of tear faults identified by Medwedeff (1992) in the subsurface, or fault scarps mapped on the surface.

Besides marking decreases in elevation from west to east along the fold crest, the wind gaps also separate segments of Wheeler Ridge that display abrupt decreases in the width of its front limb, which we relate directly to fault slip at depth according to fault-bend fold theory (Suppe, 1983). This is well illustrated in the profile of the wind gap located ~700 m west of the main water gap (Fig. 3). This wind gap is defined by a distinct, low-elevation gap in the ridge crest (Fig. 4) and is coincident with a tear fault constrained by subsurface structural contours (Medwedeff, 1992). The northern end of the valley terminates at the front limb of the fold. Comparison of the valley's profile, and the profile of the ridges on either side of the valley, shows the relative magnitude and distribution of uplift before and after it was abandoned (Fig. 9).

For this wind gap, we interpret the difference in the width of the front limb as being equivalent to the amount

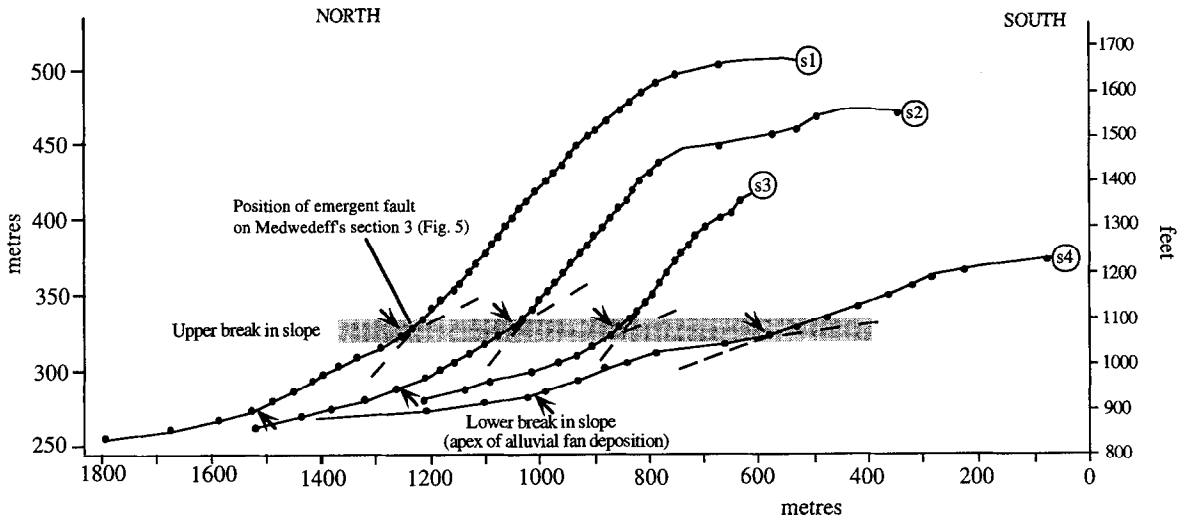

Fig. 7. Topographic cross-sections across the ridge on either side of the aqueduct wind gap The change in slope near the base of the front limb of the fold is the location of the emergent north-directed thrust which accommodates shortening in the uppermost levels of the fold.

of fold growth while the valley was being actively cut downward. The difference in height between the elevation of the plunge panel lying west and east of the drainage represents the vertical, east-facing relief across the tear fault that underlies the valley, whereas the elevation of the valley relative to the present-day rivers crossing the anticline gives the amount of uplift since the stream valley was abandoned. The difference between the valley profile and that of the ridge on either side yields the uplift which occurred on either side of the drainage before it was abandoned.

Two water gaps currently transfer sediment across Wheeler Ridge from the hinterland of the thrust belt (Shelton, 1966; Zepeda *et al.*, 1991, 1996; Medwedeff,

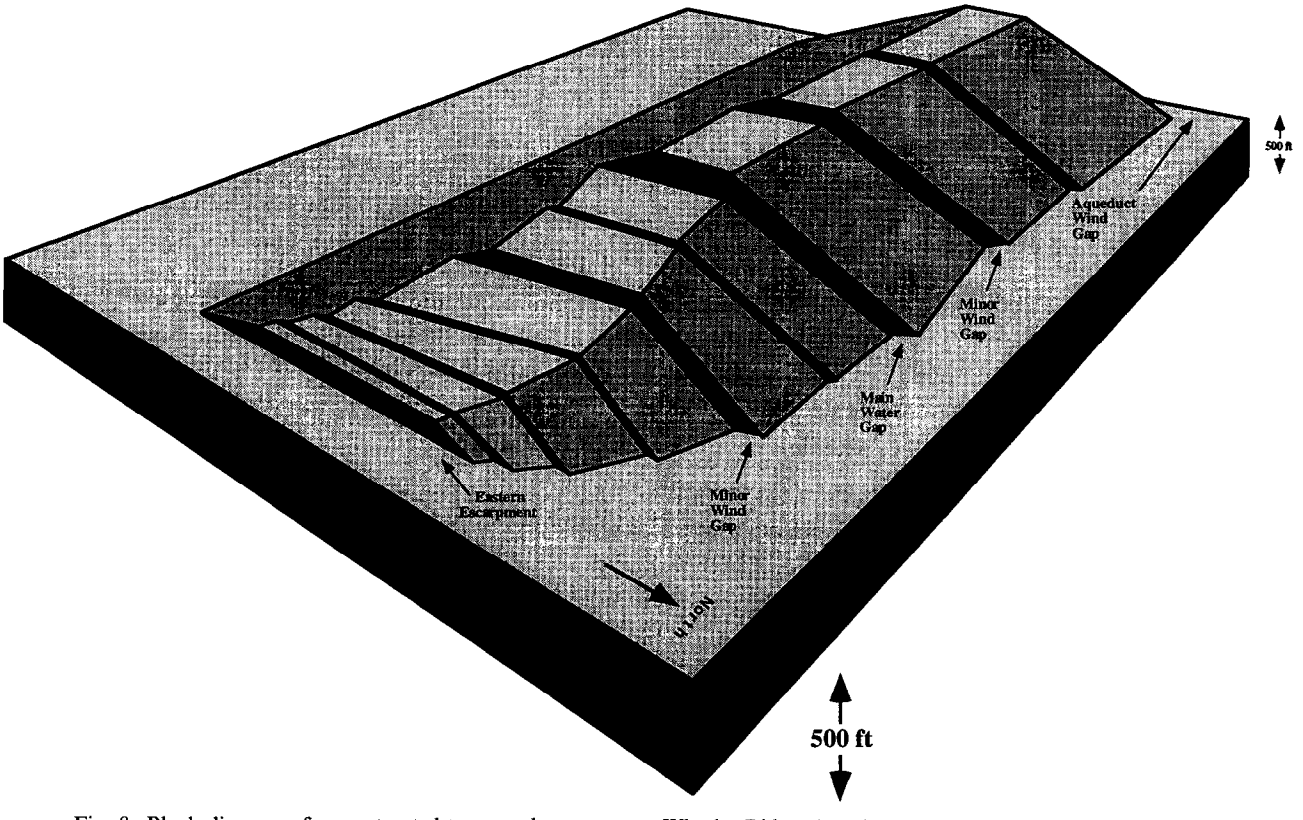

Fig. 8. Block diagram of reconstructed topography on eastern Wheeler Ridge viewed towards the southwest. Diagram is constructed by projecting flat-lying segments of the plunge panel across wind and water gaps, and by locating the edges of fold limbs based on the morphology of the fold and the cross-sections of Medwedeff (1992). Greater uncertainty exists from east to west, where the fold becomes progressively more eroded. Note the coincidence of tear faults with large amounts of dip-slip with major transverse drainages which occupy wind and water gaps.

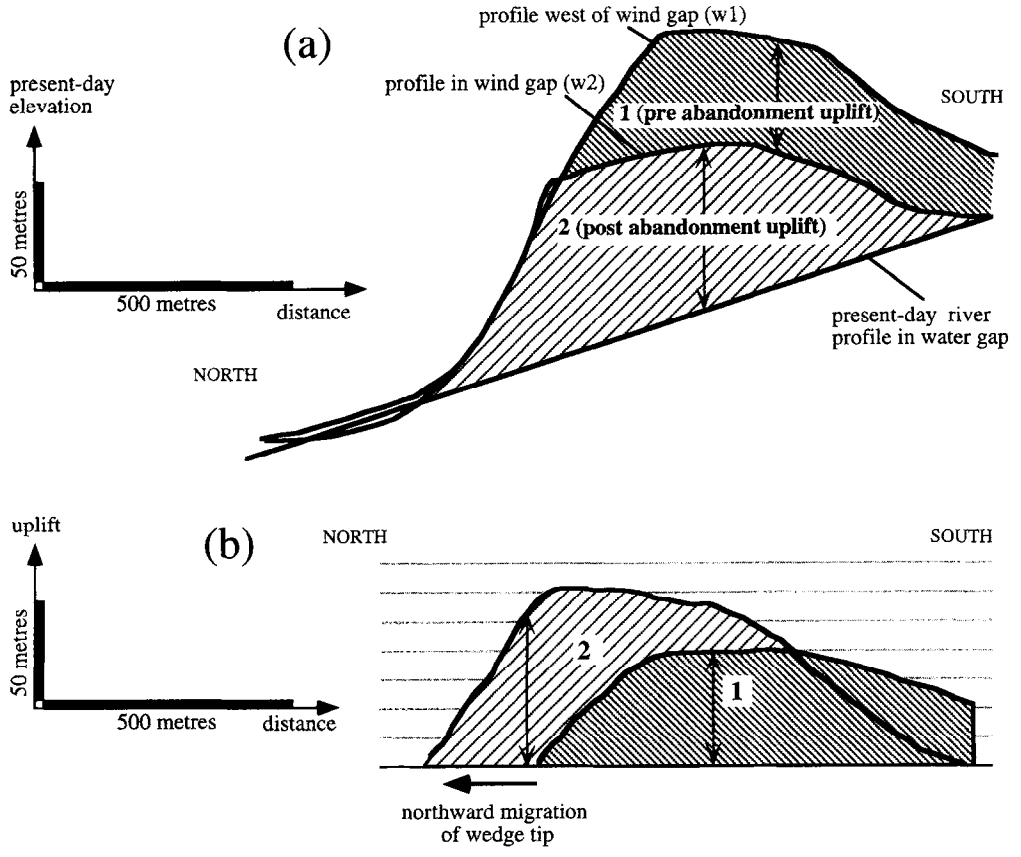

Fig. 9. (a) Topographic cross-sections in the vicinity of the wind gap in the central ridge-segment through which a sequential uplift history was obtained. The locations of the cross-sections are indicated on Fig. 3. The first period of uplift was responsible for the difference in topography between the wind gap and adjacent parts of the ridge, once the profile of the water gap is restored to that of the present-day river (i.e. the regional slope). A second episode of uplift is recorded by the difference in slope between the abandoned wind gap and the regional slope. A final period of uplift resulted in uplift of the northern part of the eastern and central ridge-segments. (b) Sequential distribution of uplift which has produced the central part of the ridge.

1992; Burbank and Verges, 1994). The main water gap forms a steep-walled canyon between the central and eastern portions of the fold that is also coincident with a tear fault constrained by structural contours (Medwedeff, 1992). This drainage system has maintained a regional gradient across the fold. The water gaps are incised into younger strata than the aqueduct and other wind gaps located further west, and thus by inference are younger features.

We interpret the formation of new water gaps to be dependant on patterns of stream capture in the hinterland of the thrust belt, south of Wheeler Ridge (see also Burbank *et al.*, 1996). Headward erosion and incision of younger, more easterly drainages captures flow from more westerly drainage systems that traverse the older, more uplifted parts of the fold (Burbank and Verges, 1994; Burbank *et al.*, 1996; Fig. 3). As flow is diverted further east, stream power and downcutting diminish until continued uplift isolates the incised valley. Subsequent folding uplifts the water gap further, producing a wind gap from what was earlier a transverse drainage capable of maintaining a regional gradient across the fold.

STRUCTURAL IMPLICATIONS OF GEOMORPHIC FEATURES

Kink band migration

The surface morphology of Wheeler Ridge strongly supports the assertion of Medwedeff (1992) that kink-band migration is the dominant deformation mechanism that acts to build the fold. This is particularly evident upon examination of the character of the front limb where it widens in a self-similar fashion across progressively deformed older deposits (Fig. 8). The sharply curved fold hinges bounding the north and south edges of the fold crest also support this mechanism, particularly on the uneroded eastern segment (Fig. 3). In addition, the geometry of Wheeler Ridge conforms to models of plunging fault-bend folds where the western section has reached a maximum stage of uplift termed a crestal widening stage (Shaw *et al.*, 1994; Fig. 8). The central and eastern segments were correspondingly also uplifted during an early stage of crestal uplift, which is associated with consumption of the undeformed fold crest. The plunge panel reflects this relationship where it widens in

accordance with decreasing amounts of fault slip to the east (Medwedeff, 1992; Shaw *et al.*, 1994; Fig. 8). The younger age of the plunge panel and fold limbs which form the eastern end of Wheeler Ridge is also apparent from less well developed soils (Zepeda *et al.*, 1996) and poorly developed drainage networks (Fig. 3).

Continuity of fault geometry

Mapping on aerial photographs indicates the south-dipping emergent thrust can be continuously traced from the aqueduct wind gap to halfway across the eastern segment of the fold (Fig. 3). This thrust is best defined in the subsurface near the water gap where its increased displacement apparent in the subsurface suggests it forms the top of a south-directed wedge (Medwedeff, 1992). This fault has also been identified in a gravel quarry on the crest of the eastern segment of the fold, where it cuts the ground surface 500 m south of the base of the front limb apparent on the surface. The well-defined front limb on the eastern segment of the fold therefore lies in the footwall of the emergent thrust and thus did not develop in response to fault bend folding above it.

We suggest therefore that the double wedge geometry better defined further west, where repetition of stratigraphic section in boreholes is greater and more apparent in the subsurface, extends eastward to nearly the end of the fold. In this interpretation, the front limb on the eastern segment has formed above a north-vergent thrust wedge which accommodates the bulk of shortening in the eastern segment of the ridge, similar to the geometry of the fold further west (Fig. 5). The north-vergent thrust in the upper levels of the fold exposed in the quarry (Zepeda *et al.*, 1996) is interpreted to be a relatively minor thrust which does not in itself record the full amount of shortening across the structure. Alternatively, available subsurface data from the western fold segment permit an interpretation where the north-vergent thrust offsets the ground surface at the base of the front limb of the fold (Medwedeff, 1992) while a south-vergent backthrust transfers some slip back to the south. The other north-vergent thrust that is exposed in the gravel quarry (Zepeda *et al.*, 1991, 1996) is then be considered to be another fault splay extending upwards from the basal south-dipping thrust.

Lateral propagation

Lateral propagation of eastern Wheeler Ridge is clearly defined by the morphology of the fold, the progressively younger age of less folded deposits from west to east and the elevation of valley floors in the wind and water gaps (Shelton, 1966; Zepeda *et al.*, 1991, 1996; Medwedeff, 1992). The present morphology of Wheeler Ridge suggests that its eastern termination has been fault-bounded throughout its history for the last $\sim$125 ka.

We interpret the east-facing fault scarps to record the former eastern terminus of the fold as it propagated from west to east for the following reasons. The east-facing faults are, in general, progressively less eroded and hence younger from west to east. Fault scarps consistently face east, which can be kinematically related to the geometry of the blind thrusts and also, to the high angular shear strains that have been calculated along the fold (Medwedeff, 1992).

Based on these geomorphic and structural relations, patterns of fold propagation can then be reconstructed assuming that each scarp once recorded the eastern terminus of Wheeler Ridge and that they become progressively younger from west to east. Evidence for the stepped nature of the crest of the fold (Figs 4 & 8) then implies that lateral propagation of Wheeler Ridge is episodic (Medwedeff, 1992) and the fault tip has remained stationary while significant amounts of fault slip were added to the thrusts. Based on a simplified model of reconstructed topography (Fig. 8) that links the north-vergent thrusts with the tear faults, we predict that the tear faults will be oblique with a right-lateral component of slip. In this model, the throw on the north-vergent thrusts is equivalent to the vertical separation across the tears, while the heave on the thrusts corresponds to the right lateral component of slip on the tear faults. A search for laterally displaced landforms, such as incised stream channels and alluvial fanheads, did not yield obvious geomorphic piercing points across the east-facing scarps. However, the minor amount of diplacement across these faults may preclude the development of these features, which have previously been identified on more deeply incised, longer-lived fault scarps.

The model also predicts the tear faults are only active while they bound the eastern end of the fold; they become inactive once eastward propagation on the thrusts occurs. Other kinematic implications of the model indicate that the tear faults will terminate at the top of the back limb of Wheeler Ridge. Based on our examination of the largely uneroded eastern segment of the fold, the tear faults terminate in this location (see also Fig. 8).

Incremental fold growth

Although a historic seismic event has not occurred on any of the thrusts that drive uplift of Wheeler Ridge, we suggest that the fold grows incrementally by episodic events caused by earthquakes. Wheeler Ridge lies in an area which contains seismically active thrusts, as indicated by paleoseismic events defined in trench excavations across both the Pleito Thrust (Hall, 1984), and on the emergent, south-dipping thrust that accommodates shortening in the upper levels of Wheeler Ridge anticline (Zepeda *et al.*, 1991, 1996). Also, the 1952 M7.6 Arvin–Tehachepi earthquake, which occurred on the underlying White Wolf fault (Stein *et al.*, 1988), is a recent thrust-type seismic event in this region. There is also increasing evidence from other active fold and thrust belts that fault-related folds grow during thrust-type earthquakes (Yield-

ing *et al.*, 1981; Philip *et al.*, 1992; Kelson *et al.*, 1996). In addition, unique terraced landforms which are preserved on the front limb of Wheeler Ridge have been hypothesized to form during earthquakes on the north-vergent thrust wedge at depth (Mueller and Suppe, 1997).

Available age constraints do not permit detailed documentation of individual folding events which act to build Wheeler Ridge. However, a more detailed examination of plunge panel morphology yields insights into the episodicity of fold growth and lateral fault propagation. Tear faults localized on the plunge panel of Wheeler Ridge accommodate most of the relief from west to east along the fold and point to the styles of earthquake-related fault rupture patterns that may be occurring here. We suggest that several general end-member modes of earthquake-related faulting behaviour may act to build plunge of fault-bend folds and displacement on blind thrusts (Fig. 10), although not necessarily lateral propagation. These include: (1) slip events on thrusts with similar displacements along strike that terminate abruptly at tear faults, build displacement over multiple earthquake cycles and then step eastward to form a new tear (Fig. 10a), (2) slip events with gently decreasing displacement along strike that may or may not accommodate lateral propagation (Fig. 10c) and (3) slip events on thrusts that do not extend completely to the end of the fold and do not accommodate lateral propagation (Fig. 10b).

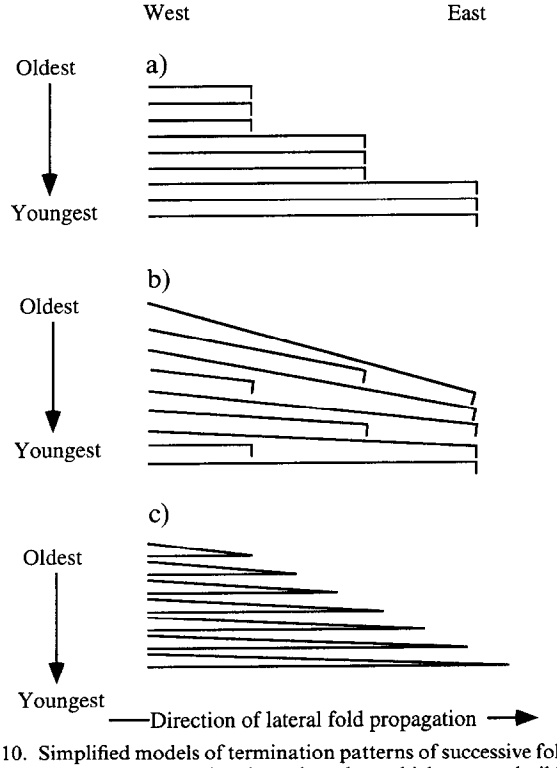

Fig. 10. Simplified models of termination patterns of successive folding events caused by thrust-related earthquakes which act to build the eastward plunge of Wheeler Ridge. (a) Illustrates the pattern we interpret to be the dominant process which creates the geomorphic features we observe. In this scenario, eastward plunge of the fold is produced by folding events that progressively step eastward after occupying a single position along the structure for multiple earthquake cycles. Tear faults with large displacement are formed by this process, in addition to wind and water gaps. (b) Illustrates a more random temporal pattern of fold terminations that does not act to build large tear faults or other evidence for lateral propagation of the fold. (c) Illustrates a pattern of folding where individual events have gently decreasing uplift towards the termination of the fold, which does not create large displacement tear faults but should create wind and water gaps.

Alternative (1) is interpreted to produce the bulk of earthquake-related growth of Wheeler Ridge because tear faults appear to accommodate most of the change in relief along the structure and there is abundant geomorphic, soil and isotopic evidence (Zepeda *et al.*, 1996) that points to lateral propagation of the fold. This is also supported by historic surface ruptures produced along thrusts that decrease abruptly towards fault segment boundaries (Philip *et al.*, 1992). Slip produced in alternative (2) likely plays a lesser role in growth of the fold in our view, because tear faults are not required by the model, but clearly play an important role in uplift at Wheeler Ridge. Alternative (3) requires formation of tear faults, but is also unlikely to be a dominant process at Wheeler Ridge because of the strong geomorphic evidence for lateral propagation of the fold.

The ratio of fault displacement vs fault length

The tear faults accommodate along-strike changes in uplift of the fold (Figs 4b & 11). The sense of displacement across the tear faults indicates that uplift of the fold cumulatively increases away from the fault tip. Such differential uplift will steepen the plunge panel on the fold crest and increase the angular shear strain along the structure (Medwedeff, 1992). Studies of fault populations have established the relation

$$D = cL^{1\text{-to-}2} \quad (1)$$

where D is the maximum fault displacement near the centre of the fault, L is the length of the fault rupture, and c is a constant (Walsh and Watterson, 1988; Gillespie *et al.*, 1992; Cowie and Scholz, 1992a; Dawers *et al.*, 1993).

Thus,

$$D/L = cL^{0\text{-to-}1} \quad (2)$$

which implies that the displacement gradient (D/L) increases as the fault length (L) increases, as long as the exponent exceeds zero. This displacement gradient (D/L) represents a zone from near the centre of the fault to the fault tip. It does not refer to displacement gradients in close proximity to the fault tip, which may evolve in a different manner as the fault tip migrates (Cowie and Scholz, 1992b). Assuming that changes in lateral displacement gradients on subsurface thrust faults result in lateral changes in limb width in fault-bend folds, this relation produces the observed rate of increase in structural relief seen along the length of Wheeler Ridge (Fig. 4c). Alternatively, variation in lateral displacement gradient may result from barriers to propagation at relay

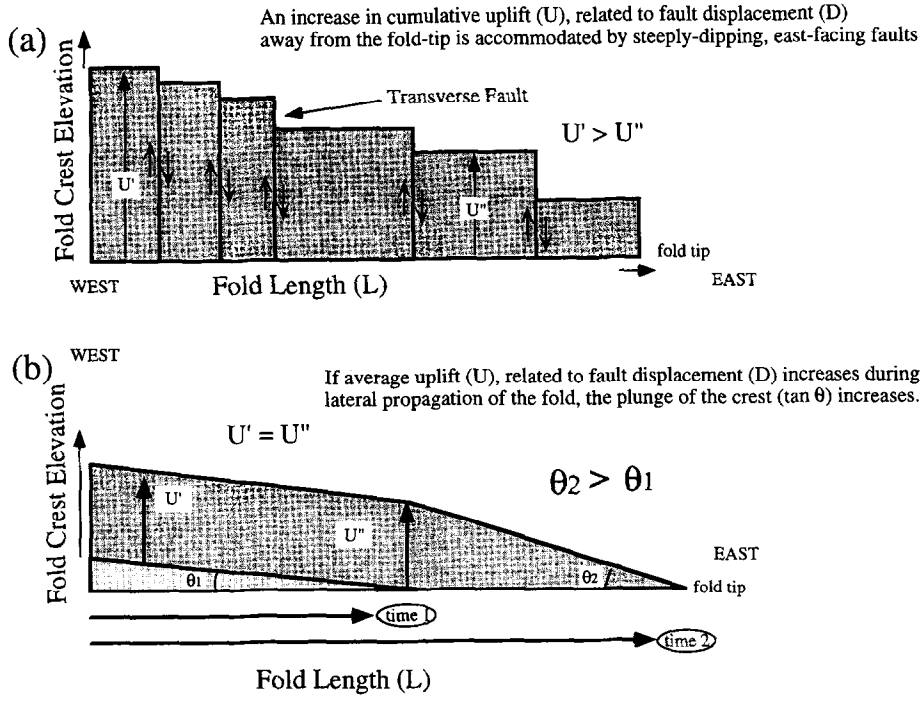

Fig. 11. Illustration of the relation between uplift and the length of Wheeler Ridge. (a) Cumulative uplift increases to the west because of the longer period of active shortening there. Abrupt variation in uplift is accommodated by east-facing tear faults. (b) Illustrates how the inclination of a plunge panel increases as rates of lateral propagation decrease.

ramps formed between separate fault segments (Trudgill and Cartwright, 1994).

Medwedeff (1992) calculated that fold-tip migration rates at the Wheeler Ridge are five times the rate of fold-crest uplift. The topographic gradient of the youngest fold tip (in the vicinity of East Salt Creek) is substantially lower (Figs 3 & 4) than that of the older fold comprising the central part of the ridge (and occuring in the vicinity of the West Salt Creek). We interpret this to suggest that the 65 ka–present day history of fault propagation has been mechanically easier than the period from 65 to 125 ka.

The dimensions of geological structures at Wheeler Ridge are unusual. The along-strike extent of individual fault-segments comprising the fold (~3 km) is anomalously short, with distances of between 5 and 15 km more commonplace. In addition, the relief on the central and western parts of the ridge is relatively high, producing particularly steep gradients (Talling, 1994). Also, the topographic expression of closely-spaced tear faults is not commonly observed at the terminus of other growth folds, although in most cases the topographic expression of these folds are highly dissected (Talling, 1994). More importantly, in a few locations in which detailed subsurface data are available (Woodring *et al.*, 1940; Maher *et al.*, 1975) structural contours also fail to pick out tear faults. Thus, it appears that the formation of closely spaced tear faults by the Wheeler Ridge thrust system is relatively unusual.

We interpret the unusually short length of fault segments comprising Wheeler Ridge, the steep gradient for its plunge panel (i.e. high D/L ratio) and the abundant tear faults to be a result of an upper crustal stress regime that may be higher than average for many other fold and thrust belts. Rapid crustal shortening in this portion of the northern Transverse Ranges is clearly related to a major restraining bend in the San Andreas fault. This, coupled with the realization that thrust faults in strike-slip restraining bends may rupture coevally during large magnitude earthquakes in southern California (Baljinnyam *et al.*, 1993; Bayarsayhan *et al.*, 1996; Mueller and Suppe, 1997) suggests that strain rates for the northern Transverse Ranges fold and thrust belt may be high in comparison to other contractile fold and thrust belts. Indeed, calculation of fault slip for the latest Quaternary (i.e. post 14 ± 3 ka) history of shortening at Wheeler Ridge yields rates of *ca* 10 mm yr^{-1} (e.g. Mueller and Suppe, 1997), a value exceeded by only a few major strike-slip faults in southern California. Alternatively, we envisage pore fluid pressure to play an important role in determining faulting behaviour on nearly flat-lying blind thrusts. Therefore, regional low pore fluid pressures in the area of Wheeler Ridge could also effectively act as a barrier to lateral fault propagation.

For shorter periods of fold growth (i.e. for the central and eastern segments), the formation of especially large tear faults is inferred to be in response to an increase in rock strength governed by lithology that coincides with an increase in the sand/shale ratio at the level of the basal décollement (Medwedeff, 1992). This may affect lateral variation in pore fluid pressure resulting in the overall slow rate of lateral propagation of Wheeler Ridge indicated by its high D/L ratio.

CONCLUSIONS

Geomorphic landforms produced by active folding and lateral propagation of Wheeler Ridge, such as drainage networks, fault scarps, fold limbs and transverse drainages, indicate that the eastern part of the fold is being uplifted above a northward moving wedge along most of its exposed length. Mapping of emergent back thrusts developed at higher structural levels suggests that a double wedge geometry extends eastward to nearly the end of the fold, an extension to previous interpretations (Medwedeff, 1992). Available geomorphic and age data permit the interpretation that emergent thrusts offset progressively younger growth sediments from west to east, which corresponds to patterns of lateral propagation of the fold caused by slip on underlying blind thrusts. Development of wind gaps in transverse drainages is interpreted to be related to a decrease in stream flow, caused by headward capture by younger drainage networks southeast of Wheeler Ridge which develop as the fold grows laterally.

Construction of a kinematic model that is consistent with fault-bend fold theory (Suppe, 1983) and the present geometry of the fold (Zepeda *et al.*, 1991, 1996; Medwedeff, 1992) permits the geometry and sense of slip on transverse faults to be related to the migrating lateral termination of the fold. The model and comparison of observed fault scarps and plunge panel(s) suggest that Wheeler Ridge grows laterally by slip events with nearly similar displacement along strike that terminate abruptly at tear faults. Subsequent shortening builds displacement over multiple earthquake cycles and then the thrust steps eastward to form a new tear fault. Although piercing points are not available to test all the predictions of the kinematic model, the tear faults are interpreted to be oblique-dextral in nature, and active only while they bound the end of the fold. Tear faults with particularly large displacements are associated with the lateral variation in lithology at the level of the basal décollement (Medwedeff, 1992). Lateral pinchout of décollement horizons (Medwedeff, 1992) may have hindered lateral fault-tip migration at such localities.

The ratio between fault displacement and length on the blind thrusts underlying Wheeler Ridge is unusually high. We interpret this as having two possible causes: elevated strain rates caused by shortening across rapidly converging upper crust in a major restraining bend formed along the strike-slip San Andreas fault, and/or local variation in pore fluid pressure. Comparison of fault length vs displacement over the last 125 ka indicates a relative increase in rates of lateral propagation which may be equated with either a decrease in fault slip rates, or an increase (from west to east) in the pore fluid pressure in shale horizons where the basal blind thrust is located. Alternatively, the high D/L values for Wheeler Ridge may be related to relationships between fault length and displacement observed in other fault populations (Walsh and Watterson, 1988; Gillespie *et al.*, 1992; Cowie and Scholz, 1992a; Dawers *et al.*, 1993). This indicates that increasing strain gradients near fault-fold tips should be general features of laterally migrating thrust-generated folds. However, observation of other active thrust-related folds indicates that the formation of closely spaced tear faults during lateral fault migration may be relatively unusual.

Acknowledgements—The authors greatly appreciate the assistance of M. D. Stewart, J. Verges, and D. W. Burbank during field work at Wheeler Ridge. M. D. Stewart also provided detailed information on lateral migration of fault tips. R. Knipe, R. Collier, R. W. H. Butler, M. R. Leeder, and T. Elliot are thanked for comments on earlier drafts of this manuscript, while D. Medwedeff, R. Ratliff and B. Treadgill provided careful and constructive reviews. E. Keller kindly discussed recent field work on the ridge. The Dale Poe Development Corporation is thanked for allowing access to Wheeler Ridge.

REFERENCES

Baljinnyam, I., Bayasgalan, A., Borisov, B. A., Cisternas, A., Dem'yanovich, Ganbaatar, L., Kocketkov, V. M., Kurushin, R. A., Molnar, P., Philip, H. and Vashchilov, Y. (1993) Ruptures of major earthquakes and active deformation in Mongolia and its surroundings. *Memoirs of the Geological Society of America* **181**, 1–62.

Bayarsayhan, C., Bayagalan, A., Enhtuvshin, B., Hudnut, K., Kurushin, R. A., Molnar, P. and Olziybat, M. (1996) 1957 Gobi-Altay, Mongolia, earthquake as a prototype for southern California's most devastating earthquake. *Geology* **24**, 579–582.

Birkeland, P. (1984) *Soils and Geomorphology*. Oxford University Press, New York

Bloch, R. B., von Huene, R., Hart, P. E. and Wentworth, C. M. (1993) Style and magnitude of tectonic shortening normal to the San Andreas fault across Pyramid Hills and Kettleman Hills South Dome, California. *Bulletin of the Geological Society America* **105**, 464–478.

Burbank, D., Meigs, A. and Brozovic, N. (1996) Interactions of growing folds and coeval depositional systems. *Basin Research* **8**, 1–25.

Burbank, D. W. and Verges, J. (1994) Reconstruction of topography and related depositional systems during active thrusting. *Journal of Geophysical Research* **99**, 20281–20297.

Cowie, P. A. and Scholz, C. H. (1992) Displacement–length scaling relationship for faults: data synthesis and discussion. *Journal of Structural Geology* **14**, 1149–1156.

Cowie, P. A. and Scholz, C. H. (1992) Growth of faults by accumulation of seismic slip. *Journal of Geophysical Research* **97**, 11085–11095.

Dawers, N. H., Anders, M. H. and Scholz, C. H. (1993) Growth of normal faults: Displacement–length scaling. *Geology* **21**, 1107–1110.

Ekstrom, G., Stein, R. S., Eaton, J. P. and Eberhart-Phillips, D. (1992) Seismicity and geometry of a 110-km-long blind thrust fault; 1. The, 1985 Kettleman Hills, California, earthquake. *Journal of Geophysical Research* **97**, 4843–4864.

Gillespie, P. A., Walsh, J. J. and Watterson, J. A. (1992) Limitations of dimension and displacement data from single faults and the consequence for data analysis and interpretation. *Journal of Structural Geology* **14**, 1157–1172.

Hall, N. T. (1984) Late Quaternary history of the eastern Pleito thrust fault, northern Transverse Ranges, California. Unpublished Ph.D. thesis, Stanford University.

Harden, J. W. (1982) A quantitative index of soil development from field descriptions: Examples from a chronosequence in central California. *Geoderma*. **28**, 1 28.

Jackson, J. A. and Leeder, M. R. (1994) Drainage systems and the development of normal faults: an example from Pleasant Valley, Nevada. *Journal of Structural Geology* **16**, 1041–1059.

Jackson, J., Norris, R. and Youngson, J. (1996) The structural evolution of active fault and fold systems in central Otago, New Zealand. *Journal of Structural Geology* **18**, 217–234.

Keller, E. A., Zepeda, R. L., Laduzinsky, D. M., Seaver, D. B., Zhao, E. X., Johnson, D. L. and Rockwell, T. K. (1986) Late Pleistocene–

Holocene soil chronology for evaluating tectonic framework and events, transverse ranges, California. Unpublished report to U.S. Geological Survey, No. 14-08-0001-21829.

Keller, E. A., Johnson, D. L., Laduzinsky, D. M., Rockwell, T. K., Seaver, D. B., Zepeda, R. L. and Zhao, X. (1989) Tectonic geomorphology and late Pleistocene soil chronology of the Wheeler Ridge, San Emigdio Mountains and Frazier Mountains areas. Friends of the Pleistocene Field Trip Guidebook.

Kelson, K. I., Simpson, G. D., VanArsdale, R. B., Haraden, C. C. and Lettis, W. R. (1996) Multiple late Holocene Earthquakes along the Reelfoot fault, central New Madrid seismic zone. *Journal of Geophysical Research* **101**, 6151–6170.

Maher, J. C., Carter, R. D. and Lantz, R. J. (1975) Petroleum geology of Naval Petroleum Reserves No. 1, Elk Hills, Kern County, California. *U.S. Geological Survey Professional Paper* **912**, 103.

Medwedeff, D. A. (1988) Structural analysis and tectonic significance of late-Tertiary and Quaternary, compressive growth folding, San Joaquin Valley, California. Unpublished Ph.D. thesis, Princeton University.

Medwedeff, D. A. (1989) Growth fault-bend folding at Southeast Lost Hills, San Joaquin valley, California. *American Association of Petroleum Geologists Bulletin* **73**, 54–67.

Medwedeff, D. A. (1992) Geometry and kinematics of an active, laterally propagating wedge thrust, Wheeler Ridge, California. In *Structural Geology of Fold and Thrust Belts*, eds S. Mitra and G. W. Fisher, pp. 1–28. The Johns Hopkins Studies in Earth and Space Sciences **5**.

Mueller, K., and Suppe, J. (1996) Growth of Wheeler Ridge anticline, California: Implications for short-term folding behaviour during earthquakes. *Journal of Structural Geology* **19**, 383–396.

Namson, J. and Davis, T. L. (1988) Seismically active fold and thrust belt in the San Joaquin Valley, central California. *Bulletin of the Geological Society of America* **100**, 257–273.

Philip, H., Rogozhin, E., Cisternas, A., Bousquet, J. C., Borisov, B. and Karakhanian, A. (1992) The Armenian Earthquake of 1988 December 7: faulting and folding, neotectonics and palaeoseismicity. *Geophysics Journal International* **110**, 141–158.

Seaver, D. B. (1986) Quaternary evolution and deformation of the San Emigdio Mountains and their alluvial fans, Transverse Ranges, California. Unpublished M.A. thesis, Santa Barbara, University of California.

Shaw, J. H. and Suppe, J. (1994) Active faulting and growth folding in the eastern Santa Barbara Channel, California. *Bulletin of the Geological Society America* **106**, 607–626.

Shaw, J. H., Hook, S. C. and Suppe, J. (1994) Structural trend analysis by axial surface mapping. *Bulletin of the American Association of Petroleum Geologists* **78**, 700–721.

Shelton, J. S. (1966) *Geology Illustrated.* Freeman, San Francisco.

Stein, R. S. and Ekstrom, G. (1992) Seismicity and geometry of a 110-km-long blind thrust fault, 2. synthesis of the 1982–1985 California earthquake sequence. *Journal of Geophysical Research* **97**, 4863–4865.

Stein, R. S., King, G. C. P. and Rundle, J. B. (1988) The growth of geological structures by repeated earthquakes, 2. Field examples of continental dip-slip faults. *Journal of Geophysical Research* **93**, 13319–13331.

Stewart, M. D. (1996) The effect of fault growth and fault geometry change on drainage development and sediment flux in the active extensional Basin and Range province, U.S.A. Unpublished Ph.D. thesis, Leeds University.

Suppe, J. (1983) Geometry and kinematics of fault-bend folding. *American Journal of Science* **283**, 684–721.

Talling, P. J. (1994) Sedimentation and tectonic geomorphology in areas of active tectonic compression. Unpublished Ph.D. thesis, Leeds University.

Trudgill, B. and Cartwright, J. (1994) Relay-ramp forms and normal-fault linkages, Canyonlands National Park, Utah. *Bulletin of the Geological Society of America* **106**, 1143–1157.

Unruh, J. R. and Moores, E. M. (1992) Quaternary thrusting in the southwestern Sacremento Valley, California. *Tectonics* **11**, 192–203.

Walsh, J. J. and Watterson, J. (1988) Analysis of the relationship between displacements and dimensions of faults. *Journal of Structural Geology* **10**, 239–247.

Woodring, W. P., Stewart, R. and Richards, R. W. (1940) Geology of the Kettleman Hills oil field, California. *U.S. Geological Survey Professional Paper* **195**.

Yielding, G., Jackson, J. A., King, G. C. P., Sinval, H., Vita-Finzi, C. and Wood, R. M. (1981) Relations between surface deformation, fault geometry, seismicity and rupture characteristics during the El Asnam (Algeria) earthquake of 10 October 1980. *Earth and Planetary Science Letters* **56**, 287–304.

Zepeda, R. L., Keller, E. A. and Rockwell, T. K. (1991) Active folding and reverse faulting in the western Transverse Ranges, southern California: Part VIII Tectonic geomorphology of Wheeler Ridge. *Guidebook for 1991 Geological Society of America Annual Meeting*, San Diego, California, 37–45.

Zepeda, R. L., Keller, E. A., Rockwell, T. K. and Ku, T. L. (in press) Active tectonics and soil chronology of Wheeler Ridge, Southern San Joaquin Valley, California. *Bulletin of the Geological Society of America*, in press.